

An experiment to measure the electron–ion thermal equilibration rate in a strongly coupled plasma

This article has been downloaded from IOPscience. Please scroll down to see the full text article.

2006 J. Phys. A: Math. Gen. 39 4347

(<http://iopscience.iop.org/0305-4470/39/17/S06>)

View [the table of contents for this issue](#), or go to the [journal homepage](#) for more

Download details:

IP Address: 171.66.16.101

The article was downloaded on 03/06/2010 at 04:19

Please note that [terms and conditions apply](#).

An experiment to measure the electron–ion thermal equilibration rate in a strongly coupled plasma

J M Taccetti, R P Shurter, J P Roberts, J F Benage, B Graden,
B Haberle, M S Murillo, B Vigil and F J Wysocki

Los Alamos National Laboratory, Los Alamos, NM 87545, USA

E-mail: taccetti@lanl.gov

Received 19 September 2005, in final form 18 November 2005

Published 7 April 2006

Online at stacks.iop.org/JPhysA/39/4347

Abstract

We present the most recent results from an experiment aimed at obtaining the temperature equilibration rate between ions and electrons in a strongly coupled plasma by directly measuring the temperature of each component. The plasma is formed by heating a sonic gas jet with a 10 ps laser pulse. The electrons are preferentially heated by the short pulse laser (we are aiming for $T_e \sim 100$ eV), while the ions, after undergoing very rapid (sub-ps timescale) disorder-induced heating, should only reach a temperature of 10–15 eV. This results in a strongly coupled ion plasma with a $\Gamma_{ii} \sim 3$ –5. We plan to measure the electron and ion temperatures of the resulting plasma independently during and after heating, using collective Thomson scattering for electrons and a high-resolution x-ray spectrometer for the ions (measuring Doppler-broadened absorption lines). Theory indicates that the equilibration rate could be significantly lower than that given by the usual weakly coupled model (Landau–Spitzer) due to coupled collective modes present in the dense plasma.

PACS numbers: 52.27.Gr, 52.25.Fi

(Some figures in this article are in colour only in the electronic version)

1. Introduction: strongly coupled plasmas

The coupling strength of a plasma is characterized by the *Coulomb coupling parameter*

$$\Gamma_{ij} = \frac{Z_i Z_j e^2}{a_{ij} k T}, \quad (1)$$

where a_{ij} is the average particle separation between species i, j . When $\Gamma \geq 1$, the particular species in the plasma is said to be *strongly coupled* [1, 2]. This parameter can be understood as a ratio of the Coulomb potential energy to the thermal energy of the species in question, so that the potential energy dominates in the strongly coupled regime. These types of plasmas

share more properties with liquids than gases due to these strong correlations among particles, and are difficult to diagnose due to their high density and short timescales ($\sim 10^{19} \text{ cm}^{-3}$ and fs to ps, respectively, in our case).

Approximations used to derive basic plasma physics parameters such as λ_D (Debye length) and $g = 1/(n\lambda_D^3)$ break down when applied to strongly coupled plasmas, making them inapplicable. For example, $a/\lambda_D = \sqrt{3\Gamma}$ and the interparticle distance becomes $\sim \lambda_D$ for $\Gamma \geq 1/3$. As density is increased, one quickly runs into the unrealistic situation of having one or fewer particles inside a Debye sphere.

The thermal equilibration (or relaxation) rates between ions and electrons in strongly coupled plasmas are also very different from those of ideal plasmas. Coupled collective modes of the ions reduce these rates compared to the Spitzer rate [3]. Dharma-wardana and Perrot [4] have calculated relaxation rates of a dense two-temperature aluminium plasma to be more than an order of magnitude lower when the relaxation occurs as an interaction between normal modes of each species rather than between the individual particles.

Even at these reduced rates, thermal equilibration between electrons and ions is expected to occur on timescales of < 1 ns, such that fast, high resolution diagnostics are required to distinguish this rate from the Spitzer rate (which predicts equilibration in ~ 300 ps). What follows is a description of the experimental set-up used to form the plasma and how we plan to diagnose it.

2. Experimental arrangement

We form the plasma by rapidly heating an SF₆ sonic gas jet with a 10 ps, ~ 1 J laser pulse focused down to a 200 μm spot size located ~ 1 mm under the jet nozzle (ID = 660 μm , OD = 902 μm). The beam preferentially heats the less massive electrons (we are aiming for $T_e \sim 100$ eV), leaving the ions at room temperature but highly ionized, resulting in $\Gamma_{ii} > 1$. Ions should undergo rapid disorder-induced heating (DIH) to ~ 10 eV [5], making our $\Gamma_{ii} \sim 5$ at the start of the temperature equilibration phase between the electron and ion systems. (DIH of the ions occurs in timescales of order $1/\omega_{pi} \approx 200$ fs [6], and is over by the time we begin our measurement of electron–ion relaxation.) We intend to measure the ion and electron temperatures independently as a function of time. We use collective Thomson scattering to measure the electron temperature and Doppler-broadened absorption spectroscopy, using a high-resolution spectrometer, to measure the ion temperature.

2.1. Laser beams and experimental set-up

The gas jet is aimed downwards, and the heater beam intersects the jet below the nozzle at right angles to the gas flow. Two other beams are then used to diagnose the plasma: the Thomson scattering (TS) and the x-ray generation (XG) beams. Figure 1 shows a top view of the vacuum chamber (in the lower left-hand corner), the heater and diagnostic beams, and the location of the collection optics. The three beams enter the experimental area at the top of the figure. The TS beam is in the same plane as the heater and oriented at 84° from it, while the XG beam is out of the plane and aimed upwards onto a solid target behind the plasma.

Collective Thomson scattering as a function of time is obtained by focusing the TS beam into the plasma and collecting the scattered light at 174° from incidence, passing it through a spectrograph and streaking it with respect to time. We obtain the electron temperature by measuring the separation between the two frequency-shifted scattered peaks. The TS beam is synchronized to the heater beam by locking the oscillators of each to within 2 ps of each other. An optical trombone is used to vary the TS delay relative to the heater.

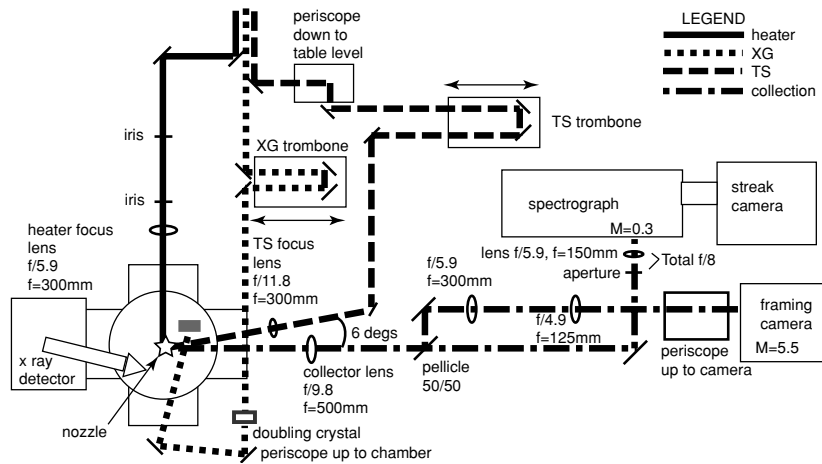


Figure 1. Top view of experimental set-up. Solid line: heater (527 nm, 10 ps, 1 J); dotted: x-ray generating (XG) (527 nm, 600 fs, 500 mJ); dashed: Thomson scattering (TS) (532 nm, 120–150 ps, 100 mJ); dash-dot: collection optics.

The XG beam hits a solid target about 10 cm behind the plasma (a tungsten substrate coated with molybdenum disulfide) to generate backlighting x-rays. These pass through the plasma and under the right conditions ($T_e \sim 100\text{--}300$ eV, where the S^{XV} population is large enough to cause absorption but low enough to avoid opacity broadening effects) are absorbed by the plasma and diffracted by a quartz Bragg crystal into a detector. The XG beam is split from the heater beam and therefore automatically synchronized—its relative delay to the heater is varied with an optical trombone.

2.2. Plasma target characterization

We characterized the SF_6 gas jet using a Mach-Zehnder interferometer. The variation in neutral gas density was studied as a function of time from the firing of the gas valve for a given backing pressure. Figure 2 shows an interferogram taken at the time the heater laser is fired, well past the point when the flow has reached a steady state.

Analysis of the interferogram provides a plot of the neutral density as a function of distance r from the axis at $z = 1$ mm below the nozzle. These curves are fit to the analytical density $n(r, z) = A + n(0, z) \exp[-(r/\Delta r)^2]$, and a density scale length of $\Delta r = 0.93$ mm is obtained. The Gaussian radial density profile agrees with [7] and is expected for a fluid flow into vacuum. A molecular density of $1.8 \times 10^{18} \text{ cm}^{-3}$ is found near $r = 0$. The existing gradient below the nozzle is not desired, but is a consequence of operating the gas jet in the sonic rather than supersonic regime [8] to get the desired density of SF_6 gas.

2.3. Alignment procedure

In order to ensure reproducible results, we align both heater and TS beams to a $150 \mu\text{m}$ pinhole drilled into a diffusively reflecting copper plate. This pinhole target, mounted on a kinematic mount, is positioned relative to the nozzle using an x - y translation stage and magnified onto a monitor using a CCD camera. The target is placed at a slight angle to the heater beam to reflect both heater and TS beams diffusively onto our collection optics (figure 1). The heater beam is first aligned to the pinhole using our streak camera in focus mode. The pinhole is then

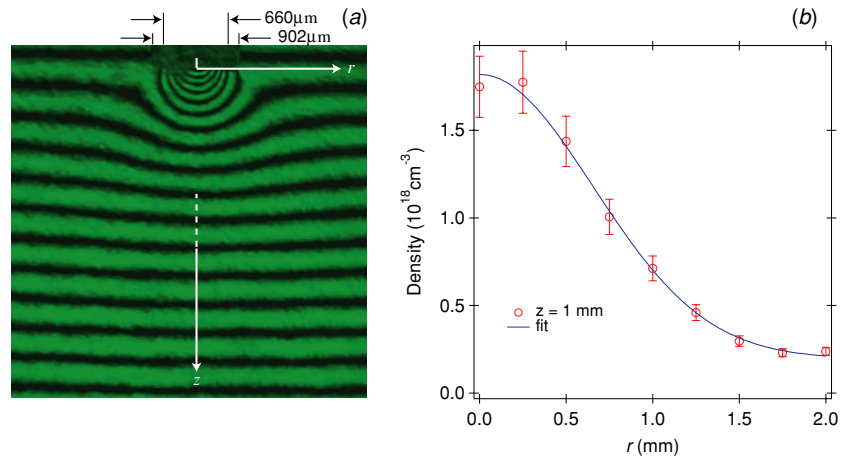


Figure 2. Mach-Zehnder (a) interferogram of SF₆ gas jet and (b) analysis showing density as a function of r at $z = 1 \text{ mm}$.

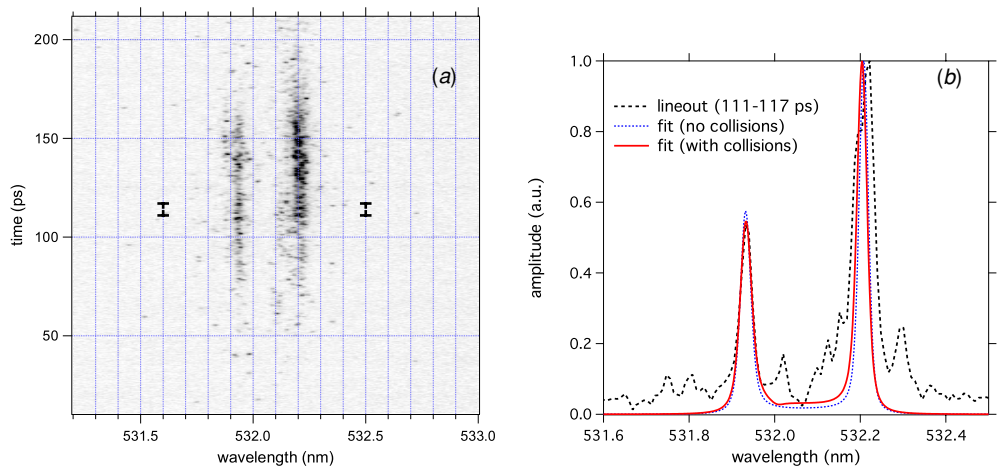


Figure 3. Thomson scattering (a) signal (lineout range delineated) and (b) lineout (dashed) and fit including (solid) and excluding (dotted) collisions. Both include instrumental response of 0.4 \AA .

moved to the location desired for Thomson scattering, and the TS beam and the collection optics are focused and aligned to this location.

We also take a 5 ns time-integrated picture of the plasma during our shots. The plasma location varies with the location of the heater beam focus. Normally one focuses past the nozzle to obtain the best plasma breakdown. Gradients in the plasma make it difficult to predict exactly where the plasma will break down for varying parameters, but it is reproducible as long as these are maintained constant.

3. Results

So far we have obtained T_e using Thomson scattering and are still finalizing the ion temperature diagnostic. A typical Thomson scattering signal and lineout are shown on figure 3. The

Thomson scattered signal is streaked for 200 ps. The spacing between the peaks is 0.27 nm, indicating an electron temperature of ~ 40 eV using the simple estimate

$$\frac{\omega_{\text{iaw}}}{k_{\text{iaw}}} = c_s \cong \sqrt{\frac{\bar{Z}kT_e}{m_i}}, \quad (2)$$

and assuming that the signal comes predominantly from Fluorine ions that are ionized to $Z = 7$. This is consistent with a Saha calculation of Fluorine charge state fraction versus T_e assuming $n_i = 1.05 \times 10^{19} \text{ cm}^{-3}$. A multi-ion species fitting routine derived from [9] has been developed that includes collisional energy transfer effects as per [10], and results are shown in figure 3(b). The fit results in T_e and T_i of 39 eV and 15 eV, respectively. We use the Mermin functional form with collision frequencies for electron–ion and ion–ion given by [11]. Collisional effects are minimal, as shown in figure 3(b).

4. Discussion

We are currently working on increasing our plasma temperature, in conjunction with dealing with the density gradients existing in the gas jet and plasma that result in non-uniform TS signals. We are also in the process of characterizing an x-ray absorption spectrometer designed to measure the ion temperature.

References

- [1] Ichimaru S 1982 *Rev. Mod. Phys.* **54** 1017
- [2] Murillo M S 2004 *Phys. Plasmas* **11** 2964
- [3] Spitzer L 1962 *Physics of Fully Ionized Gases* (New York: Interscience)
- [4] Dharma-wardana M W C and Perrot F 1998 *Phys. Rev. E* **58** 3705
Dharma-wardana M W C and Perrot F 2001 *Phys. Rev. E* **63** 069901
- [5] Murillo M S 2001 *Phys. Rev. Lett.* **87** 115003–1
- [6] Killian T C *et al* 2005 *Plasma Phys. Control. Fusion* **47** A297
- [7] Behjat A, Tallents G J and Neely D 1997 *J. Phys. D: Appl. Phys.* **30** 2872
- [8] Malka V *et al* 2000 *Rev. Sci. Instrum.* **71** 2329
- [9] Sheffield J 1975 *Plasma Scattering of Electromagnetic Radiation* (New York: Academic)
- [10] Mermin N D 1970 *Phys. Rev. B* **1** 2362
- [11] Huba J D 2004 *NRL Plasma Formulary* (Washington: Naval Research Laboratory) pp 33–4